269 Wind Turbine Issues in Germany

Jörg E. E. Seltmann[*]**and Tim Böhme**
Deutscher Wetterdienst

October 11, 2017

1. Introduction

Wind turbines (WT) have long been known to adversely affect radar measurements. Due to their huge radar cross section, WT cause clutter both from contributions inside and outside the radar main beam and multi-path effects as well as so-called "shadowing" effects behind the WT. These effects are highly variable in time and space due to varying WT operations and atmospheric conditions. They are reflected in the electromagnetic field distribution around the WT, scanned by the radar and propagate through the radar processing chain into base data, such as reflectivity, radial wind and dual polarisation moments, and further on into follow-up products and algorithms. The latter comprise rain accumulation, model assimilation, and warning products such as warnings of thunderstorms, hail, or mesocyclones, just to name a few. Thus, the relevance of WT effects depends on the application of the radar data.

Accordingly, several methods have been proposed on protection against WT interference. To our knowledge, none of them has solved the problem so far. Particularly, no operational tools are available to reliably identify, quantify and/or appropriately mitigate these wind turbine effects. As a first step, a realtime WT identification is necessary as affected pixels are highly variable and a much larger area than just a small environment around the geographic position of a WT may be affected over time. As a second step, detailed WT sensitivity studies are necessary, in order to know the range of possible error magnitudes and to evaluate the impact of WT and of possible

Figure 1: Map of German WT sites (blue dots) as of 2017 with DWD weather radars and wind profilers. Source: BKG 2016.

---
[*]Corresponding author address: Dr. Jörg Seltmann, DWD, Meteorologisches Observatorium Hohenpeißenberg, D-82383 Hohenpeißenberg, Germany. Email: Joerg.Seltmann@dwd.de

future WT mitigation algorithms on follow-up procedures and final products. Modeling has shown that very few and even single WT pixels may impede the detection of hail or mesocyclones, and WT echoes from outside the main beam may still contribute significantly and even surpass severe weather thresholds.

DWD operates a network of 17 C-band (incl. 16 dual-pol) weather radars. Due to a turnaround in German energy policy, more and more wind turbines (WT) have been installed, reaching a number of 26.200 in spring 2017 (Fig. 1). Over the years, their sizes have increased from early 60 m to presently 200 m total WT height, giving rise to stronger radar echoes up to higher antenna elevations. Part of them have even been erected in the near-field of the weather radars in spite of the WMO recommendation of a 20 km radar protection radius around weather radars which, as a political compromise, had been reduced to 15 km (i.e., 56% of the 20 km area) in Germany.

This contribution is to give an overview of the WT-weather radar challenge, focusing on the scope of WT impacts as observed by various network radars and on different stages of the radar data processing chain, particularly in automated procedures. A couple of ideas that have been proposed to cope with existing WT will be discussed as well.

2. WT effects in radar raw and base data

Wind turbines influence the radar electromagnetic field redistributing energy resulting at each measuring point in either more or less energy than without WT. From a radar meteorological point of view, these effects are commonly referred to as clutter (unwanted echoes) and shadowing. Multiple-body effects occur if more objects (soil, ground targets, WT, etc.) are present. The total reflected energy from within the 3 dB main lobe or outside (flanks of main lobe and side lobes) is measured in amplitude and phase of the complex raw radar time series in both horizontal and vertical polarisations. Various moments such as Z, v, ZDR, ρ_{hv}, etc. or even spectra are extracted from these raw data. In each of these moments, WT influences are reflected in a different way (see Frech and Seltmann, 2017, this volume) and propagate through the entire radar
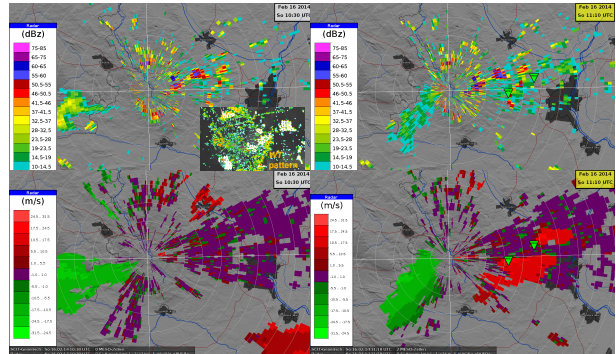

Figure 2: Reflectivity and radial wind signals of WT in the 15 km protection zone of Ummendorf radar on 16 February 2014. WT cause reflectivities up to ≥ 65 dBZ and wide areas of radial wind velocities around 0 m/s. When overlain with real weather signals (green and red precipitation areas), false dipole structures lead to non-realistic mesocyclone detections (green triangles).

processing chain. The magnitude of the WT effect on all levels depends largely on boundary conditions such as geometry, weather and operations conditions. In the following sections the WT influences on weather radar data will be further described with differentiation into single effects.

a. *Wind turbine clutter*

It is widely known that WT cause clutter, e.g. in reflectivity and wind velocity data. An example is shown in Figure 2. While reflectivity data are marked by increased values (up to a factor of 10^6), radial wind velocity shows additional non-weather echoes often around 0 m/s.

Due to the exorbitant size of WT as compared to water droplets, strong WT clutter is straightforward. Furthermore, WT are usually (but not always) arranged to form a wind park, so that extended areas may be affected. Figure 3 shows extreme wind park interference created by a wind park 3-6 km southsouthwestwards of the Ummendorf radar. No precipitation is present. WT reflectivities exceed 46 dBZ which serves as a thunderstorm threshold at DWD; some pixels show even values larger than 55 dBZ (hail threshold). The maximum reflectivity exceeds 65.7 dBZ in the present case.
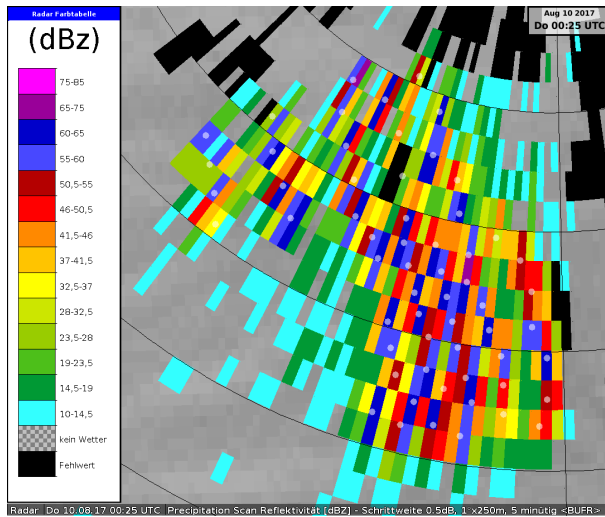
Figure 3: Doppler-filtered reflectivity data of precipitation scan of Ummendorf radar, Ausleben wind park, 10 August 2017, 00:25 UTC, without precipitation. Grayish dots indicate the positions of known WT underlaid with color coded reflectivity values.

Figure 4 shows the situation of Figure 3 five hours later, this time with widespread moderate precipitation. In this case, quality assurance deletes most WT affected range bins and creates large connected data gaps. Weather information including any interesting or even dangerous features is lost in this area and cannot be recovered. Particularly, interpolation is not appropriate.

b. *Sidelobes and flank of main beam*

As is well known, a radar does not only ′see′ what is right in front of the antenna, much as we hope so, but the total echo is the convolution integral of the antenna pattern with the echo distribution at a given distance. That is why strong echoes such as WT are detected via antenna side lobes, sometimes over wide areas. Figure 5 shows an example of sidelobes effects over a wide azimuth in the data of Neuheilenbach radar.

Figure 6 presents a severer example of WT detection from outside the main radar beam. The former wind park at Admannshagen (blue circle) at a distance of 7-8 km southwestwards to the Rostock radar was hit by the main
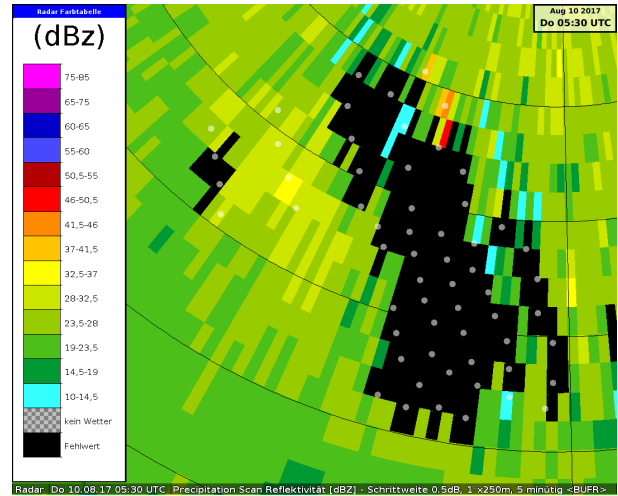

Figure 4: Widespread precipitation in Doppler-filtered reflectivity data of precipitation scan of Ummendorf radar, Ausleben wind park, 10 August 2017, 05:30 UTC. Grayish dots indicate the positions of known WT. In the data, interference has been detected by standard signal processing. Corresponding range bins have been deleted, leaving a large blank area that cannot be interpolated.

beam at 0.5° elevation only; the main beam of the precipitation scan at 1.1° passed 40 m above the wind park. Even so, massive echoes beyond the 46 dBZ severe weather warning threshold appeared at 1.1°.

c. *Repowering*

Repowering means the replacement of existing WT by larger and more powerful ones. In Germany, it is run through a public authorization procedure in which DWD has to be heard as a public agency. The wind park shown in Figure 6 underwent repowering meanwhile. The total WT height increased from 71-77 m to 149-150 m while the number of WT decreased from five to three. Exemplarily, the geometry of the two lowest sweeps relative to one of the repowered WT is given in Figure 7. Prior to permission, authority demanded a prognostic estimation of the expected WT impact after repowering. This has been effected by a simple geometric height extrapolation of observed data, not regarding the larger RQS of the new WT. In Figure 8, the expected reflectivity profile
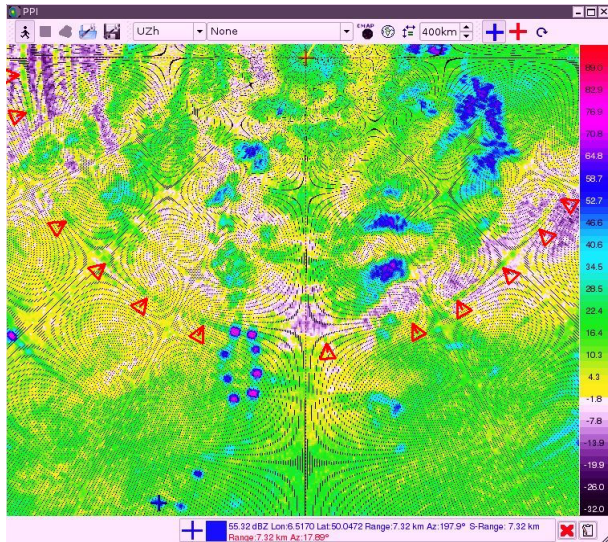
Figure 5: Several WT at close range of Neuheilenbach radar are detected via sidelobes over widespread light rain. Some of the ring segments extend over an azimuth of ∼160° (indicated by red arrowheads).
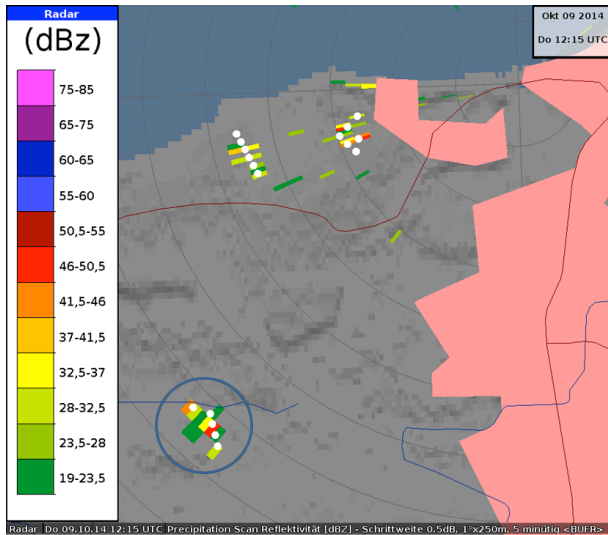

Figure 6: The former Admannshagen wind park (white dots in blue circle) at 7-8 km southwestwards of the Rostock radar creates echoes at 46 dBZ, even though the 3 dB radar beam does not hit the WT but passes about 40 m above (see Fig. 7 bottom left).
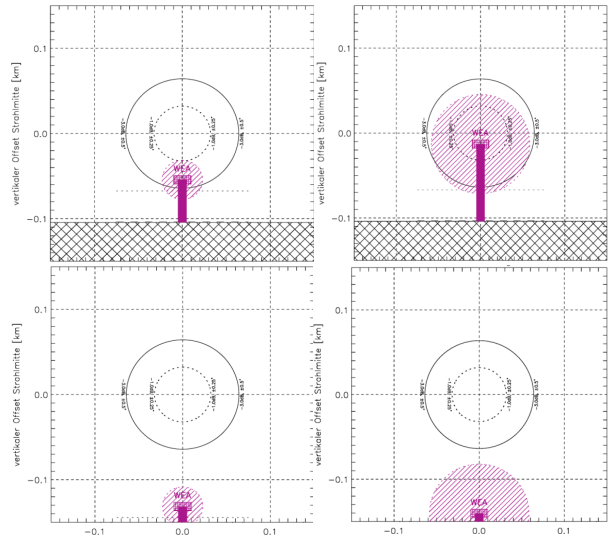

Figure 7: Overlap of radar beam cross section (defined at 3 dB, solid black line) and area covered by WT rotors (purple shading) of the lowest radar sweeps before (left) and after (right) repowering at elevations 0.5° (top) and 1.1° (bottom).
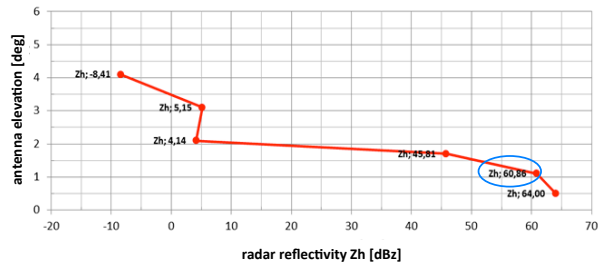

Figure 8: Forecast of vertical reflectivity profile over the planned Admannshagen repowering, see Figure 6.
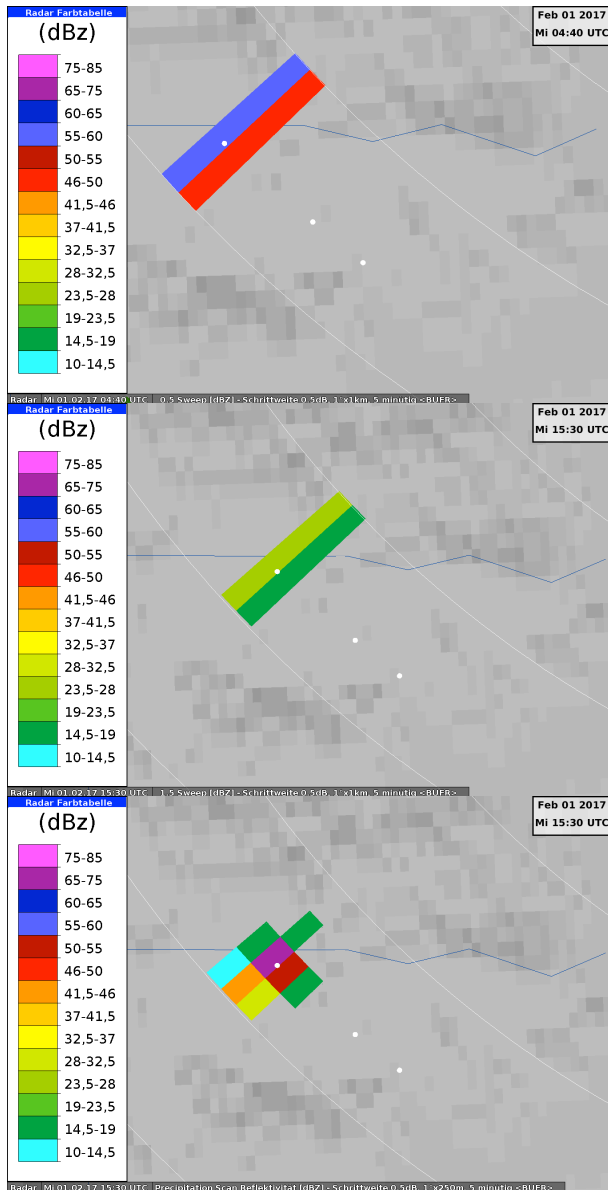
4

Figure 9: Admannshagen wind park after repowering (white dots), reflectivity measured on 01 February 2017 4:40 UTC and 15:30 UTC at elevations of 0.5° (top) and 1.5° (center) volume sweeps (both 1km resolution), and 1.1° (bottom, precipitation scan, 250 m resolution) with a maximum of more than 65 dBZ. The westernmost WT is already operating, the other two WT are not running. The 4 ring segments indicate distances 6 to 9 km from Rostock radar.
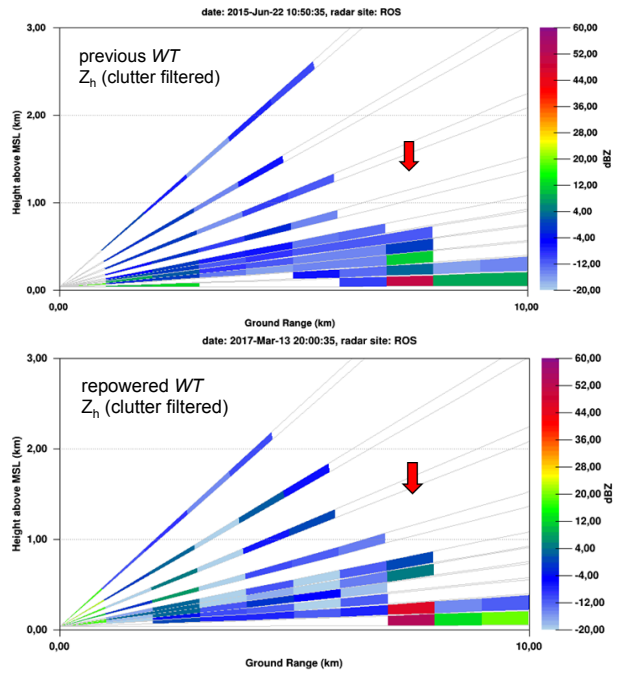

Figure 10: Top: RHI of filtered reflectivity in the direction of the previous Admannshagen wind park (arrow) which in this case is visible via sidelobes up to the fourth elevation (3.5°). Bottom: The same for the repowered Admannshagen wind park (arrow) with increased reflectivity up to the fifth elevation (5.5°), while data at 2.5° and 3.5° have been censored at this time.

$Z_h(el)$ is shown starting at the lowest elevation (volume scan at 0.5°), followed by the precipitation scan at 1.1° and higher volume elevations.

At the point of time presented in Figure 9, the former wind park (shown in Fig. 6) has been replaced, and first WT echoes are visible. WT reflectivity observed on 01 February 2017 confirms and even exceeds DWD's reflectivity expectation (see blue ellipse in Fig. 8) of more than 60 dBZ in the precipitation scan at 1.1°. Reflectivity of the northwesternmost WT is 65.3 dBZ in precipitation scan, thus surpassing the 46.0 dBZ severe weather threshold by a factor of 84. Even in the volume scan, where data have been averaged over 1 km, threshold exceedance is by a factor of 18 (58.8 dBZ measured on 01 February 2017 at 04:40 UTC).
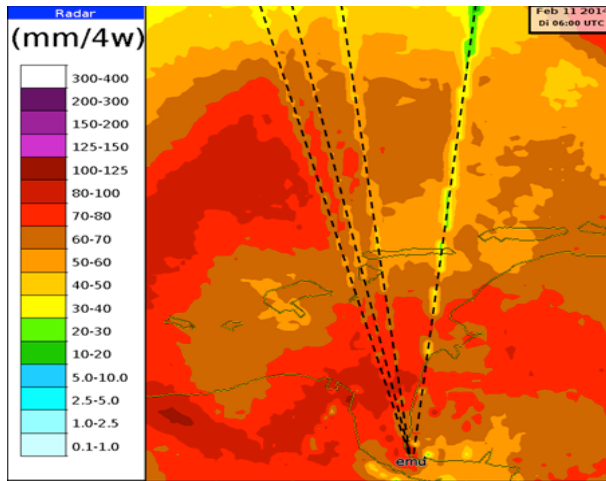
5

Figure 11: Shadowing behind 4 WT close to the Emden network radar ("emd"). The 4 week precipitation accumulation (11 January - 11 February 2014, 06:00 UTC) is reduced up to 50% as compared to unaffected surroundings.

Reflectivity RHI plots of Admannshagen wind park in Figure 10 show both clear main and side lobes WT signals in the volume sweeps of the Rostock radar. These figures show clearly the potential enforcement of WT disturbances on weather radar measurement with repowering.

It should be noted that Figures 6, 9 and 10 present Doppler filtered data. Comparing unfiltered and filtered radar data (not shown here) it turns out that the echoes of those WT with non-rotating rotors have been filtered out. Unfortunately, not all of these signals have been filtered out continuously.

d. *Shadowing*

Due to the large obstacles that WT represent, energy is lost in the radar radiation field as it propagates past the WT. Sometimes, a simple geometric shadow approximation is used to describe this type of extinction. Figure 11 demonstrates attenuation behind WT at close range from the Emden weather radar in a 4-week accumulation product. Attenuation amounts up to more than 50% as compared to unshadowed surroundings and extends to the
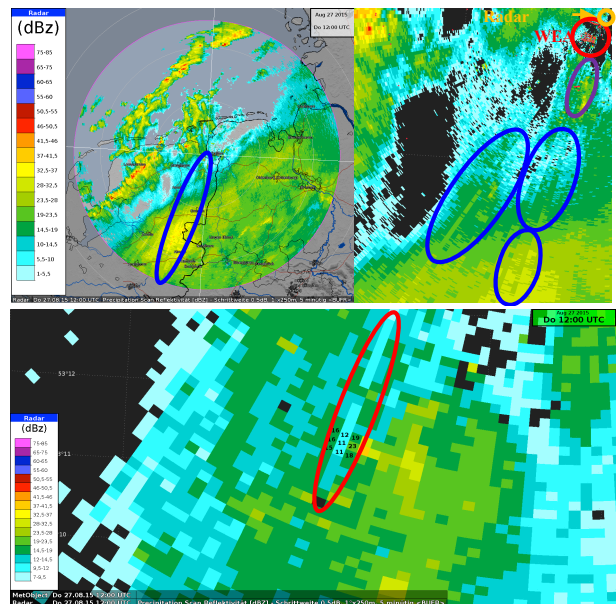

Figure 12: Reflectivity from Emden radar, precipitation scan, on 27 August 2015, 12:00 UTC. Top left: Widespread rain moving eastwards, followed by convective precipitation. Several spikes are visible extending to the limit of radar coverage. Top right: Zoom with radar and wind turbines indicated. Bottom: Further zoom with reflectivity values (in dBZ) indicated in an arbitrary "9-field".

edge of the radar coverage far into the North Sea area.

However, closer modelling shows that the simple shadow model is not always appropriate because realistically, there are more intensity minima and maxima on both sides of the zeroeth minimum that represents the geometric shadow. Moreover, the incoming wave front at the WT cannot always be considered as a plane wave originating at the radar. Interaction may occur with the ground or nearby targets such as more WT in a wind park ("three body scattering", see Fig. 13) which may be hard to explain, and still harder to model. Figure 12 shows an complex example of shadowing southwestwards of the Emden radar. Starting behind a group of WT at a distance of about 7 km southsouthwestwards of the Emden radar, positive and negative spikes are clearly visible in homogeneous stratiform precipitation up to 150 km (limit
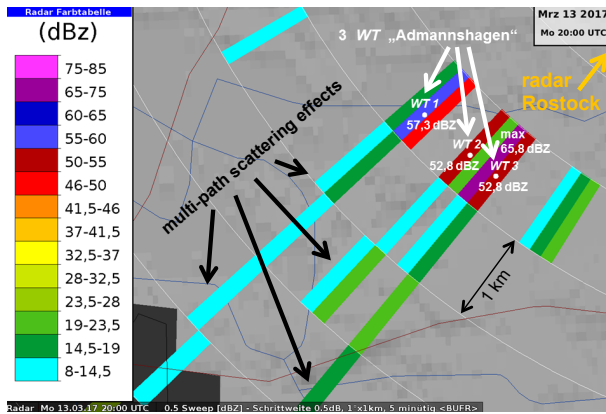
Figure 13: Multipath effect in the 0.5° volume sweep data behind the three repowered WT at Admannshagen near Rostock radar, see also Fig. 9.

of precipitation scan) and must be considered as artificial. Azimuthal range-bin differences amount to more than 5 dB at places as indicated. It should be noted that this is an instantaneous and not an accumulated example.

To our knowledge, even sophisticated diffraction calculations have not been able to model this complex situation.

e. *Multi-path effects*

Multipath effects are sometimes visible as stripe patterns in reflectivity behind WT at several German radars. An example for the repowered Admannshagen wind park is shown in Figure 13. The stripes are considered to originate from scattering between very strong targets, similarly to the well-known hail spike. Such stripes have not been observed with the prior (weaker) wind park and depend strongly on local and weather conditions. There are also observations of stripes over tens of kilometers, e.g. in the vicinity of Ummendorf radar (not shown here).

f. *Variability of WT echoes*

WT echoes are highly variable in strength, space, and time. This is a consequence of the various propagation (e.g., atmospheric refraction, multi-path scattering) and technical (e.g., side lobes) as well as WT operations (e.g., rotor state) effects. Thus, it is not sufficient to consider only the bin that geographically contains the construction

coordinates of the WT as much larger areas are stricken. Even bins/pixels many kilometers away (in azimutal, radial and vertical direction) from the WT site may be affected. Figure 14 shows the echo variation of a small wind park (4 WT) at a distance of 10 - 11 km westnorthwestwards of the Neuheilenbach weather radar together with the hit accumulation in three time steps. At this range, one pixel of 1km x 1km size is covered (at least touched) by 29 range bins, each of which is sooner or later hit. The accumulation shows that the resulting cumulative WT clutter map would exceed more than 50 individual range bins after 90 min. For a statistical analysis of the area and height that are influenced by even a small wind park see Norin (2015).

3. WT impact on radar products

Errors in base data, including missing data due to elimination of WT contaminated rang bins/pixels, propagate through the entire radar processing chain and may affect large areas. Although many severe weather warnings are issued during the convective season (e.g., thunderstorms), WT signals may influence algorithms and warnings year-round:

- Warning thresholds may be surpassed (Figs. 3, 6, 9) or missed due to WT signals (if WT pixels are cancelled as modelled in Fig. 16),

- Automated warning algorithms such as KONRAD (Figs. 15 and 16), mesocyclone detection (Figs. 2 and 18), or tornado vortex signature TVS (Fig. 18) can fail,

- Misinterpretation of base data texture including small-scale features such as hook echoes (Fig. 17),

- Effects on hydrological analysis and forecast products (QPE) also with respect to climatology (e.g., by shadowing effects, Fig. 11),

- Effects on winter warning algorithms (e.g., for the identification of areas of icy road conditions, see Figs. 19 and 20),

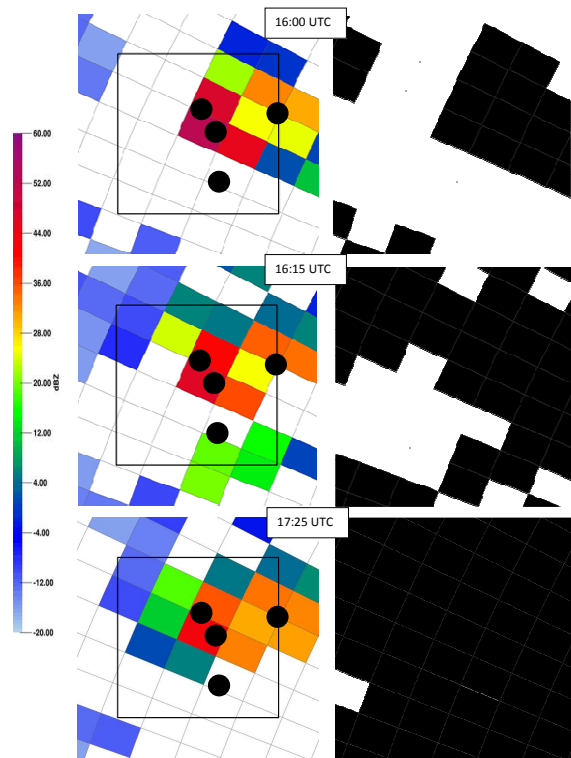- WT signals may affect combined NWP-nowcasting products, too.

7

Figure 14: Spacio-temporal echo variability of a 4 WT windpark (black dots) seen by Neuheilenbach radar. Image size is 1.5 km x 1.5 km. The thin black line indicates one 1km x 1km pixel that is sampled from 250m x 1° range bins. Left row shows instantaneous images, right side the resulting cumulative WT clutter map.

a. *Thunderstorm and hail*

Larger wind parks can easily reach and exceed both area and intensity thresholds for severe weather warnings, no matter what the particular values may be. In the case of DWD′s storm cell detection and warning system KON-RAD the thresholds are 15 contiguous pixels exceeding 46 dBZ. Figure 15 shows the reflectivity signals of an off-shore wind park 10 km south of Nysted (Baltic Sea island Lolland), 50 km northwestwards of radar Rostock on 29 June 2015, 04:10 and 04:15 UTC. WT signals cause clutter and a temporary storm cell warning object in the KONRAD product.
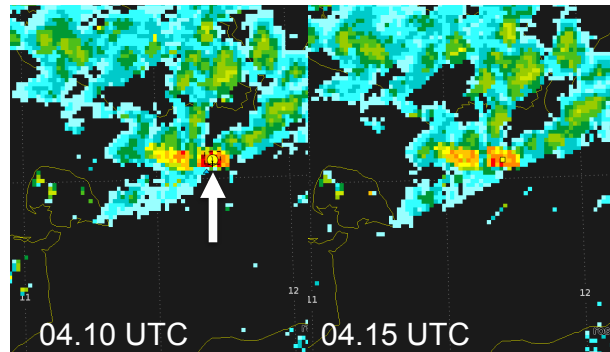

Figure 15: Two time steps of WT clutter leading to a false KONRAD cell identification (arrow) in case of Nysted wind park in the Baltic Sea at a distance of 50 km from Rostock radar on 29 June 2015.

Figure 16 presents a hail event over the city of Dresden on 15 August 2015, 13:00 UTC, together with its ESWD (European Severe Weather Database, https://www.eswd.eu) hail entry. KONRAD correctly generated a warning object of thunderstorm and hail. The figure also demonstrates in which way a very small scale WT detected in the original data base, in this case modelled by one single punched-out pixel marked in black as if by a censor map, impedes the KONRAD cell detection and, as a consequence, detection of concomitant phenomena such as hail or storm gusts. In the present case of 15 August 2015, no warning would have been issued at all.

b. *Mesocyclones and tornadoes*

In the case of threatening severe weather events such as a mesocyclone, meteorologists check the local structure of radar data particularly of the lower elevations. Using the high resolution (250 m, 5 min) precipitation scan the hook echo of a mesocyclone may be detected representing the typical signature of a mesocyclone with a high risk of a tornado. Such structures are very important for interpretation and may be masked by WT interference. Figure 17 shows the hook echo linked with a super-cell near radar Essen on 13 July 2012. The deletion of fine-scale (250 m) WT pixels as part of a hook echo could have led to a missing identification and thus to a missing warning.

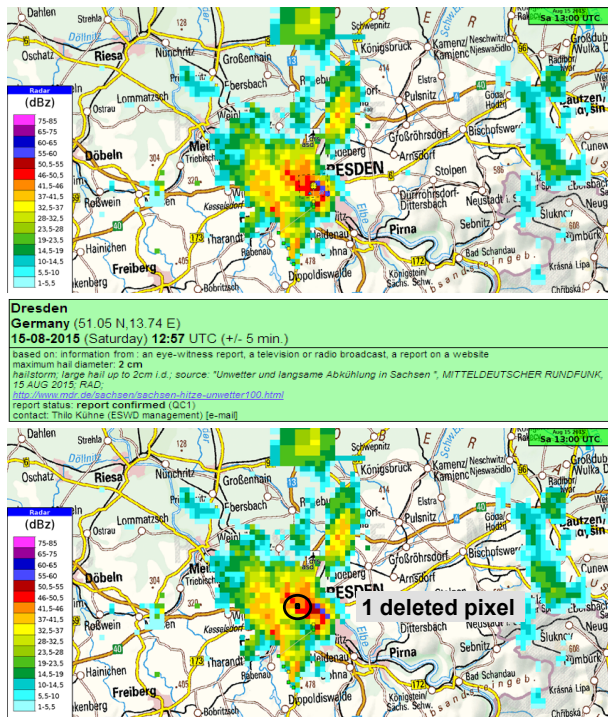Automated mesocyclone detection relies on the exis-

Figure 16: Thunderstorm that caused a KONRAD plus a hail warning over the city of Dresden (top). Center: Corresponding ESWD entry. Bottom: One single pixel has been eliminated. This model WT pixel elimination leads to the KONRAD area threshold being missed and thus to an underestimation of the hazardous situation.

tence of a cyclonic rotation dipole in polar radial wind data. Such a dipole may erroneously be detected if strong echoes create appropriate gradients in the radial wind field, as shown in Figure 2. Wide areas of radial wind velocities around 0 m/s result from WT influences. These values lead to false mesocyclone detections (green triangles) when overlain by real weather signals.

In order to estimate the risk of a tornado once a mesocyclone has been detected, the mesocyclonic rotation is scrutinized to find regions where the rotational shear is further intensified, representing the transition to a tornado. The aim is to detect a "Tornado Vortex Signature" (TVS) which is defined to be a three-dimensional circulation with its base at $0.5°$ elevation or below 600 m above radar. This definition emphasizes the significance
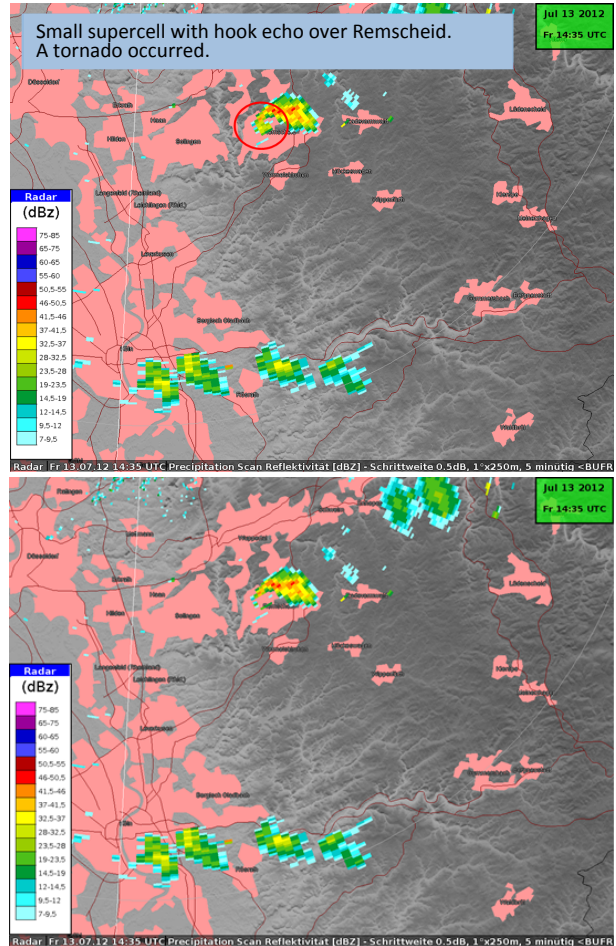

Figure 17: Top: Hook echo on 13 July 2012 over the city of Remscheid in the Rhein-Ruhr metropolitan area indicating a mesocyclone that produced a tornado. Bottom: Removal of 15 range-bins as a model of two merging "9-fields" representing two WT leads to the loss of the important hook echo signature.
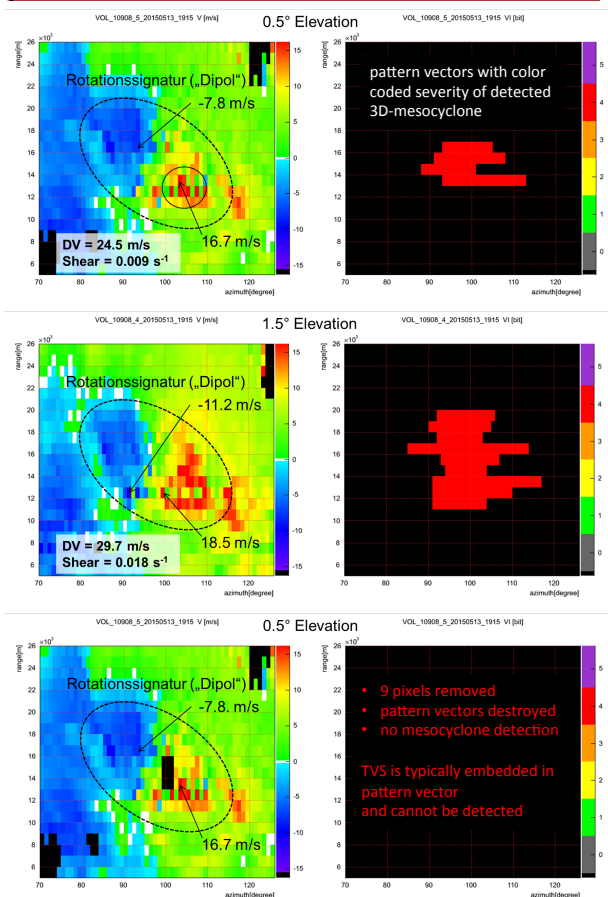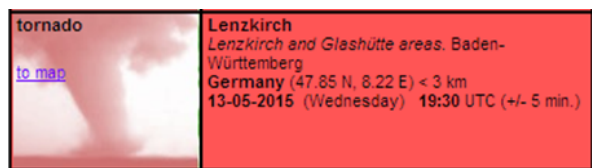
Figure 18: Rotation structure of the mesocyclone belonging to the Glashütte tornado on 13 May 2015, 19:15 UTC at the lower two elevations after subtraction of the cell displacement velocity. One pair of pixels has been marked at each elevation that together with the detection at this elevation fulfills the TVS criterion according to Mitchell. On the right hand side, pattern vectors are shown that have been used in the mesocyclone detection. In the lowest panel, 3 x 3 range bins have arbitrarily been blocked as if for a (known or detected) WT neighborhood. The upper panel shows an extract of the ESWD entry.

of the lowest elevation(s) and of measurements close to the ground. Detection of a TVS may initiate a tornado warning.

On 13 May 2015 at 19:30 UTC, tornadoes have been observed at Lenzkirch (Landkreis Breisgau-Hochschwarzwald) and at Glashütte (Landkreis Waldshut) in the state of Baden-Württemberg. DWD had issued a severe weather warning of severe thunderstorm and violent gusts at 19:01 UTC. Fortunately, there were damages only in forestal and agricultural areas. These locations are within the range of the Feldberg radar which detected the corresponding mesocyclone 15 min earlier, as illustrated in Figure 18. The rotation is superposed by convergence, leading to a skewed dipole. Moreover, there is a clear tornado vortex signature (radial velocities values indicated). The upper panel shows the ESWD entry. In the lower panel, nine range bins have exemplarily been blocked as a model of a single WT neighborhood in a WT censor map. Masking this 9-environment not only the tornado vortex signature is lost, but even the entire mesocyclone is no longer detected.

c. *Winter weather*

Sometimes it is argued that in winter time, precipitation is wide-spread and precipitation phase at surface may be determined by measured or even forecasted surface temperature, so that WT interference would have no effect because it is thought to be small scale. Figure 19 shows that this is not always the case. The upper panel presents the result of polarimetric hydrometeor classification (Steinert et al., 2013), based on the instantaneous measurement of the Türkheim weather radar on 27 January 2015 at 05:40 UTC (06:40 MEZ). At this time and place, the radar detected passing precipitation fields with relevant small scale variations in precipitation phase: Local liquid precipitation is embedded in larger intermittent snow fields (see blue pixels within red and light blue circles).

These findings are corroborated in the lower panel in Figure 19 which shows the variation with time of precipitation type as measured by a dedicated present weather sensor (disdrometer) at the Klippeneck location indicated in the upper panel. Over a time span of 6 hours, snowfall is interrupted several times by minutes of rainfall or a mixture of both while surface temperature is below 0°C. In this case, precipitation reaching the ground instanta-

Figure 20: NowCastMIX snowfall warning proposals are affected due to superposed WT signals near radar Neuheilenbach (nhb) on 21 January 2015.

Neuheilenbach radar at 16:30 UTC). Especially when WT echoes overlie weather signals (at 18:30 and 19:15 UTC), no appropriate data interpretation is possible. This affects also weather warnings, especially when issuing warnings in advanced systems with high temporal and spatial resolution.

4. Mitigation of WT interference

Clearly it is desirable to avoid WT influence as early as possible. The earliest possible avoidance is not to have WT impact at all. Maybe the impact can be minimized by siting optimization or construction measures. Once WT interference is there, it would best be removed as early as possible in the radar processing chain, while using spoiled data and discussing end product quality control is not considered to be an effective operational mitigation tool.

a. *Efforts on part of WT*

In the following, some measures in the run-up to radar or WT installation and during WT operation are listed:

i. Radar siting: Undoubtedly, the best solution would be to have a radar site available that is not infested with WT. Unfortunately, this is rarely the case, and many more siting considerations have to be taken into account, particularly in a radar network.

ii. Construction permits: Once the radar is in place, avoiding construction of new WT becomes an issue. Bilateral agreements or official regulations may help. In Germany, however, based on the alternative energy pri-
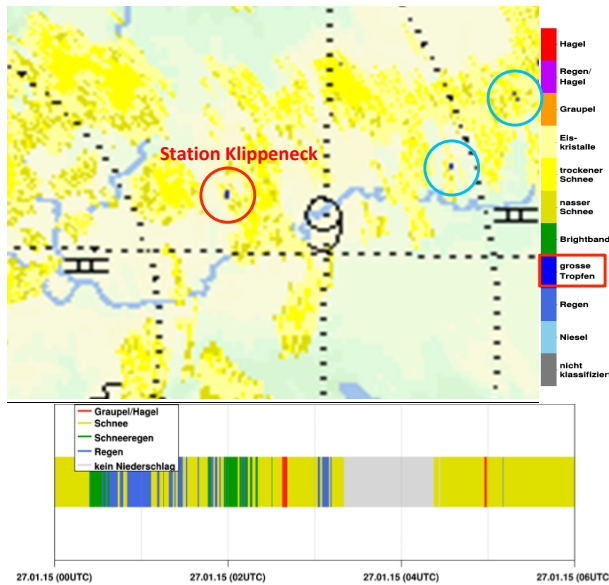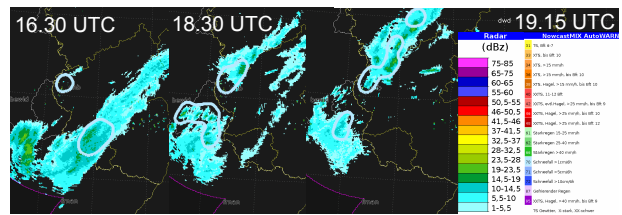
Figure 19: Top: Radar HMC over the southwestern rim of the Swabian Alb, Southern Germany, on 27 January 2015 at 05:40 UTC. Widespread snowfall (yellow pixels) with imbedded local rain (blue pixels) have been identified. The Klippeneck station is situated below the two single blue pixels within the red circle. Bottom: Precipitation phase over time as derived from disdrometer measurements at Klippeneck. This observation represents an independent verification of the radar HMC with its small-scale liquid precipitation.

neously freezes resulting in black ice which is subject to warning. That is why small-scale radar information can be decisive for warning of icy conditions where there is no ground observation.

Thus, winter precipitation is not always homogeneous and widespread. As precipitation phase may change on a small local scale, small pixel groups affected by WT may well mask the effect with a corresponding detrimental effect on warning and nowcasting.

Weather interpretation by superposed WT and weather signals is complex and challenging. In Figure 20 the automatic NowCastMIX algorithm marks heavy snowfall areas in passing precipitation fields over Southwestern Germany. While most signals are weather related, some signals base on WT echoes (see upper polygon around

ority plan of the government, each case is considered separately by the WT lobby and authorities, not taking into account the overall contamination of the region.

iii. WT arrangement: Sometimes, there is an option to choose the arrangement pattern of wind turbines in a wind park. This may be useful if WT can hide behind closer obstacles, or be arranged in one radial seen from the radar to avoid multiple-path effects and wide-spread shadowing. The effect of otherwise arranging WT is not clear.

iv. Absorbing materials: Sometimes special materials have been proposed such as built-in absorber mats or $\lambda/4$ coating. Echo mitigation of up to 10 dB has been reported, which is far too little to solve the problem. Besides, high absorption would not help with shadowing but probably create much higher attenuation than WT interference without absorbers.

v. Operations restrictions: Sometimes, construction permits are granted under operations constraints such as orders to switch-off the WT under certain weather conditions. While worth investigating, this option would not be operationally applicable unless fully automated including feedback. Moreover, the beneficial effect has not been proven yet. Particularly, because Doppler filtering and CCOR threshold would still flag the corresponding bins as not valid, as shown in the following section.

b. *Radar algorithms*

Just like with usual clutter, there are several possibilities to cope with WT clutter (not shadowing!), at least theoretically. Like clutter treatment prior to the advent of Doppler weather radar, WT clutter may be flagged by a censor map, which may be static or dynamic. In both cases, WT range bins or pixels may be removed or just be flagged. But just like modern Doppler clutter filtering, one would like to have a quantitative WT correction recovering the weather signal.

i. Censoring: Once range bins or pixels WT are known to be affected by WT they may be flagged. Thus, range bins or pixels affected by WT may be excluded from further processing. If there were enough data left at close range, adaptive sampling might be an option, depending on the application. If not, removed range bins or pixels will create a gap in the data field that may mask precipitation features and cause underwarning falling below intensity and area thresholds (Figs. 4, 16, 17 and 18). Thus, censoring may avoid overwarning but is prone to underwarning instead.

ii. WT clutter map: A simple static WT map may be created transferring known geographic WT locations to the polar radar or cartesian composite coordinate systems. One disadvantage would be that construction of a new WT or removal of an existing one are not always known to DWD. With thousands of WT in Germany, it would be hard to keep this map up to date. Still more serious, due to the high WT perturbation variability (Fig. 14) it is not clear which pixel is actually affected at a given moment. The total area affected over a long-time period that would be needed to be considered in a cumulative static map is much larger than only the rang bins or pixel(s) of the geographic WT site. If the cumulative WT clutter map of Figure 14 were to be used, not a single range bin would be left after 90 min to sample or interpolate the inner 1km x 1km pixel (black line) from. In order avoid an excessively large - or else insufficiently scarce - WT censor map, it would be more efficient to use a dynamic map, identifying range bins or pixels that are actually affected by WT during radar processing.

iii. Identification of WT interference: In order to recognise the perturbation, certain characteristics or thresholds have to be defined, preferably at a very early stage of the processing in the time series, spectra of the signal, or the moments, i.e. within signal processor. Unfortunately, again due to the high variability of WT influences, not many characteristics of WT are distinctive or can be generalised.

Still there are several standard algorithms (that are not specific about WT) that may be able to remove WT stricken range bins from the signal data stream, such as Doppler filters, clutter micro suppression, or clutter strength CCOR. Doppler filters reduce the static parts of the echo (resulting from tower, nacelle, and maybe rotors out of operation). Because of the exceeding echo strength, the corresponding range bin is usually thresholded (e.g., by CCOR, see Fig. 4). There are also some postprocessing algorithms (as described by Werner, 2012) that may

sometimes - but not always - be effective by chance. Even if they do, under operational conditions it may be hard to tell what specific algorithms caused the dynamic flagging. This becomes even more complex, if superposed by weather signal. That is why dedicated WT detection algorithms are under development worldwide.

iv. Interpolation: Next to resampling, the easiest way to replace flagged values would be 2D- or 3D-interpolation using "clean" boundary bins or pixels. This again raises the question whether those boundary bins are "clean enough". Interpolation leads to a homogenisation and thus to a deletion of heterogeneous structures. This may be acceptable for hydrologic areal precipitation and runoff calculations but not for small-scale complex meteorological structures (e.g., hail cells, Fig. 16, tornado signatures, Fig. 18).

v. Quantitative WT correction: However, it would be highly desirable to quantify the WT perturbation effects in realtime data and thus to extract the original weather signal from the total radar echo. Maintaining the texture information of the data field is an important boundary condition for the effective use of radar data, particularly in automated follow-up procedures. Actual mitigation algorithms have to fulfil this requirement. In any case, processing algorithms are time consuming, which is an issue in realtime use of radar data. No operational algorithms are unfortunately available so far.

vi. "Inpainting": An appropriate set of external information, such as NWP information or non-radar measurements, has been proposed for use to reconstruct not the radar measurement itself, but the needed meteorological information. To our knowledge, no operational realization has been published so far.

5. Summary

This contribution was to give an overview over current WT influences on weather radar data in general and on meteorological products in particular. Further discussion, research and studies are desirable and necessary in order to improve the current condition, as many questions are still open: Can model simulation reproduce such complex interaction as shown above? What is the sensitivity of each individual radar algorithm or product towards WT? Can admissibility thresholds or areas for different algorithms be defined? What may they look like? Are there technical measures at the WT to reduce clutter/absorption effectively? Can the effect be proven and guaranteed? Is there any experience how to favorably arrange WT in a wind park? Discussion on these questions and on possible WT identification or mitigation schemes is invited.

References

Frech, M. and J. Seltmann: 2017, The influence of wind turbines on dualpol radar moments and products. *38rd AMS Conf. on Radar Meteorology, Chicago, IL, USA*, number 271.

Norin, L.: 2015, A quantitative analysis of the impact of wind turbines on operational doppler weather radar data. *Atmos. Meas. Tech.*, **8**, 593–609.

Steinert, J., M. Werner, and P. Tracksdorf: 2013, Hydrometeor classification and quantitative precipitation estimation from quality assured radar data for the DWD C-band weather radar network. *36th Conf. On Radar Meteor., 16. - 20. September 2013, Breckenridge, CO, USA*, number 363.

Werner, M. and J. Steinert: 2012, New quality assurance algorithms for the DWD polarimetric C-band weather radar network. *7th Europ. Conf. on Radar in Meteor. and Hydrol.*, number NET403.